Velocity Uncertainty and Stack Power Analysis

*Jagmeet Singh**
Regional Computer Centre, ONGC,
Vadodara

singh_jagmeet@ongc.co.in

Keywords

Velocity uncertainty, Velocity analysis, Stack power

Summary

Velocity analysis from stack power or semblance plots is common, but analysis of uncertainty in determination of velocity through these methods is never done. Starting with a Ricker wavelet spread out along hyperbolae of different velocities at different depths/times and offsets, we analyze the uncertainty in our velocity determinations. We carry out this analysis for isotropic as well as anisotropic media. In the isotropic case, we also study the effect of statics on stack power. We further study stack power vs. velocity for the case in which a primary is mixed with a multiple of lower velocity, and the case of two primaries close together.

Introduction

While carrying out velocity analysis, we often encounter large blobs of semblance, or good enough stacks at various velocities (centered around some velocity) making it difficult to pinpoint the exact velocity to be picked at a given time. This motivated us to give a measure to this uncertainty and see how it behaves at different depths and offsets. We started with a Ricker wavelet spread out on hyperbolae with different parameters and see how the uncertainty varies. We define velocity uncertainty as the width of a stack power vs. velocity curve, where by width we mean the full width at 70% of the peak stack power.

Apart from the isotropic case, we considered fitting of an isotropic velocity curve (i.e. hyperbola) to the anisotropic curve with 4^{th} order NMO. In the isotropic case, we also considered the case of two close reflectors, which is often the case, in order to see how the interference of two close reflectors reflects on velocity uncertainty in our velocity determinations. Multiples interfering with primaries also affect stack power and the certainty of our velocity determinations—we study these effects.

The paper is organized as follows. We first describe the theory/methodology used by us, and then for the isotropic case, we study how stack power varies with different stacking velocities at different times and offsets. Offset-depth ratio emerges as an important parameter—so keeping it fixed, we study stack power vs. stacking velocity for different zero offset times. We then study the effect of statics on stack power and study how it changes with offset at different time levels.

This is followed by the case of two close primaries and that of a multiple interfering with a primary to see how their interference affects stack power. Finally the anisotropic case is taken up and we study how velocity uncertainty and stack power behave when we try to fit an isotropic velocity or 2^{nd} order NMO curve to the case with 4^{th} order corrections. We compare it to the case when a fraction of the correct anisotropic parameter is introduced. We next generate synthetic data and see how our predictions match with actual results.

Velocity uncertainty

Theory and/or Method

We shall use the following basic zero phase Ricker wavelet (Ricker, 1943, 1944)

$$w(t) = \left(1 - \frac{(t-t_0)^2}{\sigma^2}\right)\exp\left(-\frac{(t-t_0)^2}{2\sigma^2}\right), \quad (1)$$

which shows a wavelet centered around time t_0. The first term on the RHS is the familiar truncated $(1-\omega^2 t^2/2)$ approximation of $\cos(\omega t)$. Another more explicit way of writing the wavelet is

$$w(t) = (1 - 2\pi^2 f_m^2 t^2)\exp(-\pi^2 f_m^2 t^2), \quad (2)$$

where f_m is the peak frequency. Since we wish to spread out this wavelet centered around a hyperbola, equation (1) gets modified to

$$w(t) = \left(1 - \frac{\left(t-\sqrt{t_0^2+\frac{x^2}{v^2}}\right)^2}{\sigma^2}\right)\exp\left(-\frac{\left(t-\sqrt{t_0^2+\frac{x^2}{v^2}}\right)^2}{2\sigma^2}\right), \quad \text{------- (3)}$$

Equation(3) describes a Ricker wavelet centered around time varying with offset in a hyperbolic manner. This provides us a tool for studying the stack power or the integral of this equation over x for different velocities at say a fixed time t_0 (or around). We discuss the results for different cases below.

Equation (3) describes an isotropic medium with no ray bending effect, the most common case used by processors. Although this is an over-simplification, it continues to be most commonly used and provides a basic framework for velocity estimation. Velocity analysis involves fitting different velocity curves to this equation and seeking the one that gives maximum stack power. Suppose, we try to fit a curve with a trial velocity v' i.e.

$$t = \sqrt{t_0^2 + \frac{x^2}{v'^2}}, \quad (4)$$

and calculate the stack power for the seismogram (3). For simplicity, we ignore the first term on the RHS of equation (3) for the time being. Sum of (3) over velocity curve (4) is given by:-

$$Stack\ power(SP) = \iint \exp\left(-\frac{\left(t-\sqrt{t_0^2+\frac{x^2}{v^2}}\right)^2}{2\sigma^2}\right)\delta\left(t-\sqrt{t_0^2+\frac{x^2}{v'^2}}\right)dtdx, \quad (5)$$

where we have enforced summing over velocity curve (4) by introducing the Dirac δ function. Integrating over time leads to

$$SP = \int \exp\left(-\frac{\left(\sqrt{t_0^2+\frac{x^2}{v'^2}}-\sqrt{t_0^2+\frac{x^2}{v^2}}\right)^2}{2\sigma^2}\right)dx. \quad (6)$$

Taking care of the first term as well on the RHS of (3), this modifies to:-

$$SP = \int_0^{x_m}\left(1-2\alpha^2\left(\sqrt{t_0^2+\frac{x^2}{v'^2}}-\sqrt{t_0^2+\frac{x^2}{v^2}}\right)^2\right)\exp\left(-\alpha^2\left(\sqrt{t_0^2+\frac{x^2}{v'^2}}-\sqrt{t_0^2+\frac{x^2}{v^2}}\right)^2\right)dx, \quad (7)$$

where we have introduced the limits of integration, x_m being the maximum offset and $\alpha^2 = 1/2\sigma^2$.

Results for different cases

(A) **Isotropic Case**

Let us now work out the integral (7) for different values of t_0, x_m ,v, v' and α^2. We start out with $\alpha^2 = 3600$, t_0=3 s, x_m=6 km, v=3 km/s. Stack power vs. velocity graph is plotted in Figure 1. We see that for maximum offset of 6 km, stack power vs. velocity curve is fairly sharp with a spread (full width at 70% of maximum stack power) of roughly 200-250 m/s or 6.67%-8.3%—even this is high when this velocity uncertainty is converted to depth uncertainty. Rearranging equation (7) a bit, we can see that the important parameter (though not the only) to look out for is offset to depth ratio.

In this case it is $(2x_m/vt_0)$=4/3, where a factor of 2 has been inserted as t_0 is two way time. Let us go to

Velocity uncertainty

another extreme, where we use x_m=2 km, rest of the parameters being the same. The curve plotted in Figure 2 shows a fair amount of flattening or an increased velocity uncertainty of around 450 m/s, which as a percentage of the correct velocity of 3000 m/s is 15%.Offset to depth ratio in this case is 4/9. In Figure 3, we have further lowered the offset to 1.5 km i.e. offset to depth ratio of 1/6, a case far from ideal.

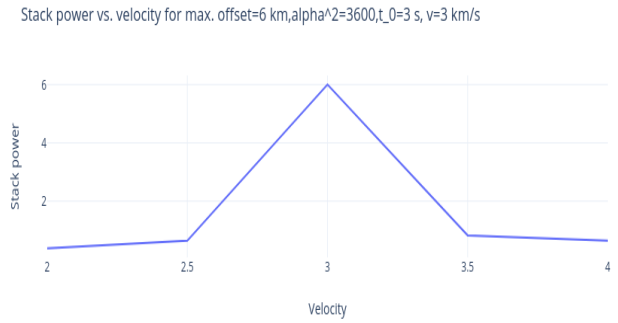

Figure 1: Stack power vs. velocity for max offset=6km,t_0=3s,v=3km/s, α^2=3600

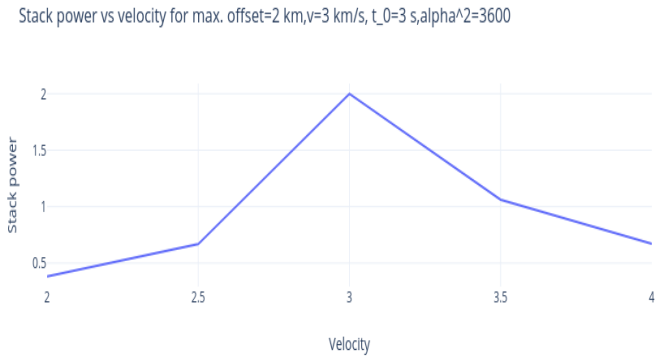

Figure 2: Stack power vs. velocity for max offset=2km,t_0=3s,v=3km/s, α^2=3600

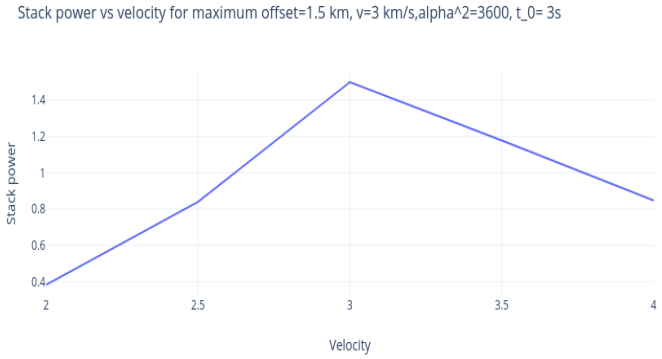

Figure 3: Stack power vs. velocity for max offset=1.5km,t_0=3s,v=3km/s, α^2=3600

As expected, the stack power curve has spread out widely making velocity determination almost impossible. Also note that the stack power curve is getting increasingly asymmetric, with greater uncertainty or spread in velocities > 3 km/s. We expect frequency of the wavelet to matter. With $\alpha^2 = 3600$, it translates to $f_m = 19\ Hz$, where f_m is the one defined in equation (2).The spectrum associated with this wavelet is shown in Figure 4. We see that this is a reasonable representation of actual frequencies encountered at the depth level indicated.

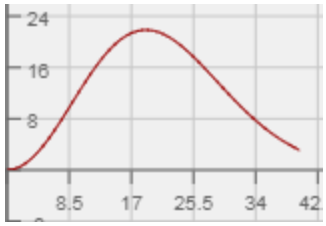

Figure 4

(A1) Effects of frequency, offset-depth ratio and time t_0

We rewrite below equation (7):-

$$SP = \int_0^{x_m} \left(1 - 2\alpha^2 t_0^2 \left(\sqrt{1+\frac{O_d^2 x^2 v^2}{x_m^2 v'^2}} - \sqrt{1+O_d^2 x^2/x_m^2}\right)^2\right) \exp\left(-\alpha^2 t_0^2 \left(\sqrt{1+\frac{O_d^2 x^2 v^2}{x_m^2 v'^2}} - \sqrt{1+\frac{O_d^2 x^2}{x_m^2}}\right)^2\right) dx,$$

--- (8)

Velocity uncertainty

where O_d is the half offset-depth ratio $\frac{x_m}{vt_o}$ .This shows that the shape of the stack power curve not only depends on frequency and offset-depth ratio, but also time t_0 and velocity ratio $\frac{v'}{v}$. We shall study below the effect of all of these. To see the effect of frequency, we use $\alpha^2 = 1800$ and $\alpha^2 = 7200$, with all other parameters(t_0, v, x_m) being the same as in Figures 1-3.

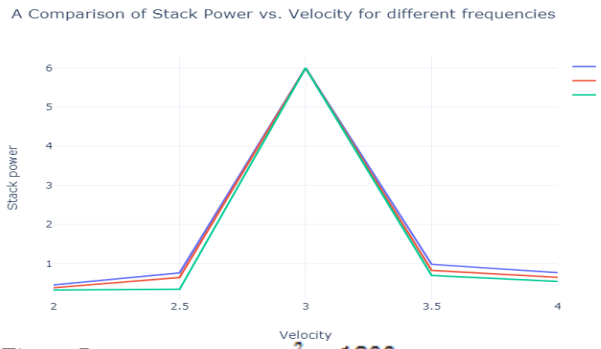

Figure 5: blue corresponds to $\alpha^2 = 1800$, red corresponds to $\alpha^2 = 3600$, green corresponds to $\alpha^2 = 7200$

Figure 5 shows results for $\alpha^2 = 1800,3600,7200$ superposed on each other. Surprisingly there is only a marginal difference in the three curves i.e. velocity spread/uncertainty is almost immune to changes in frequency at least for the parameters x_m, t_0, v used in this case.

Regarding changes with offset-depth ratio, we need to understand that it is not independent of time t_0. But we shall choose values of t_0, v and x_m, in a way that we can study the effect of t_0 and v, keeping O_d constant.

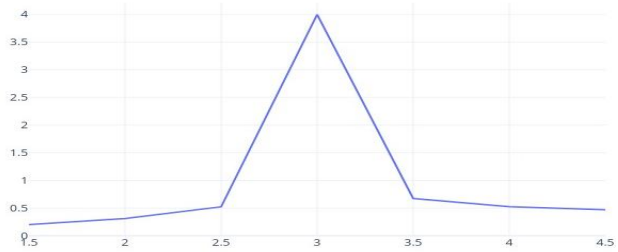

Figure 6: Stack power vs stacking velocity for $t_0 = 2s, v = 3\ kms^{-1}, offset = 4\ km$

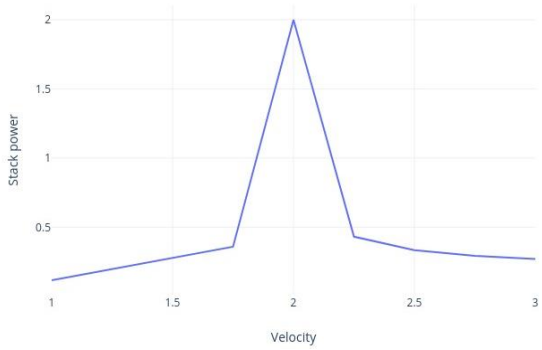

Figure 7: Stack power vs stacking velocity for $t_0 = 1.5\ s, v = 2\ kms^{-1}, offset = 2\ km$

Two such cases are shown in Figures 6 and 7—for the parameters of x_m, t_0, v chosen, we have offset-depth ratio $O_d = 4/3$, as in Figure(1). We see that velocity uncertainty as a percentage of the central velocity is highest in Figure (1), whereas it is almost same for the cases shown in Figures 6 and 7, with their zero offset times t_0 differing by only 500 ms.

(A2) Effects of statics

Velocity analysis is invariably done after application of statics to bring the data either to a flat datum or a floating datum, which is a smoothed version of the topography. While the latter is always better, processing from a flat datum is considered adequate for small static shifts, and areas without much relief. We shall study below the effect of vertical static shifts on stack power at different time levels. It is important to understand that a shifted hyperbola is no longer a hyperbola i.e. it no longer satisfies the equation of a hyperbola. For example, let us shift a hyperbola given by $t = \sqrt{\left(t_0^2 + \frac{x^2}{v^2}\right)}$ by a constant static shift Δt, so that

$$t = \sqrt{\left(t_0^2 + \frac{x^2}{v^2}\right)} - \Delta t, \qquad (9)$$

Squaring which we obtain

$$t^2 = t_0^2 + \frac{x^2}{v^2} - 2\sqrt{\left(t_0^2 + \frac{x^2}{v^2}\right)}\,\Delta t + (\Delta t)^2, \qquad \text{-- (10)}$$

which is clearly not the equation of a hyperbola. We still do velocity analysis assuming a hyperbola i.e. assuming that the effect of the last two terms in (10) is negligible for small static shifts Δt. We shall test

Velocity uncertainty

this assumption below i.e. study the effect of statics on stack power at different time levels.

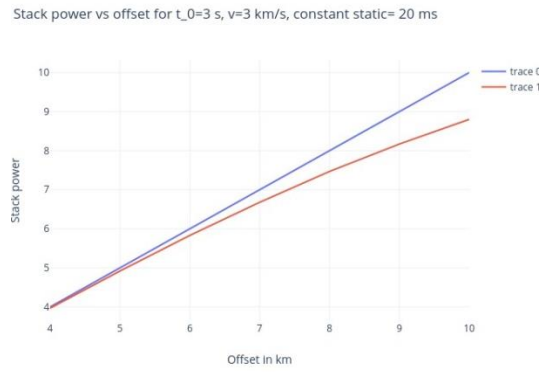

Figure 8

Figure 9

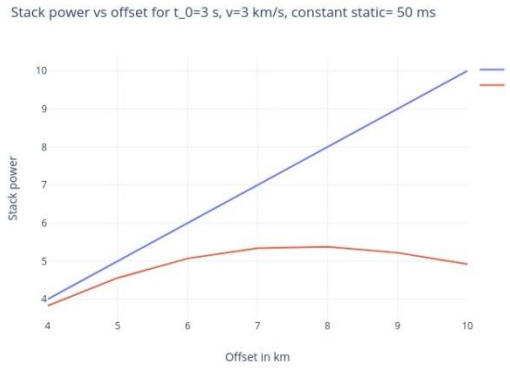

Figure 10

In Figure (8), we show loss of stack power vs. offset for a constant static shift of 20 ms for $t_0 = 3s \; and \; v = 3kms^{-1}$. We see some loss in stack power after statics (red curve). The same experiment is repeated for $t_0 = 500\,ms, v = 2\,kms^{-1}$ and the result, shown in Figure (9), shows a rapid loss of stack power with offset i.e. shallow events are adversely impacted even by a 20 ms static shift. For the case of Figure 8, if we increase the static shift to 50 ms, we again see a fast decay of stack power with offset. The results of Figures 8-10 suggest that in order to get a good stack power, we must keep static multiplied by offset to depth ratio i.e. $\Delta t. O_d$ as small as possible.

Now this is in contradiction with our previous result that O_d should be high. There is a tradeoff between velocity uncertainty on the one hand in the case without static shift, and stack power of static applied stack (with the correct velocity). Velocity analysis with short wavelength statics up to the floating datum and regional statics after NMO or migration is a better route, but in this case we should choose our replacement velocity in such a way that short wavelength statics remain small.

For the sake of completeness, we take the case of smoothly varying statics (or smoothly varying topography) by using $\Delta t = 0.02\sin(\frac{2x}{3})$ instead of the constant static of 20 ms used above. The result for $t_0 = 500\,ms, v = 2\,kms^{-1}$is shown below. This may be compared with Figure 9, which has the same parameters with constant static=20 ms. Since static is now sinusoidally varying with maximum static =20 ms i.e. statics are mostly less than 20 ms, the loss of stack power with offset is less rapid, but still appreciable.

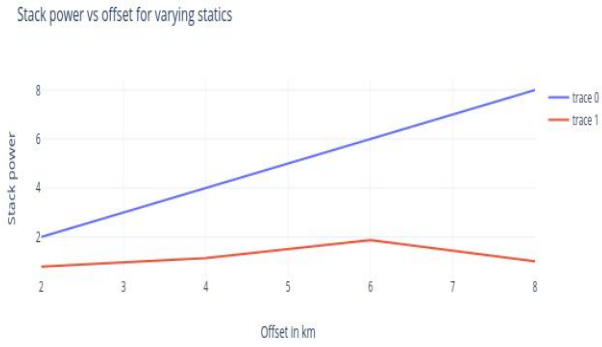

Figure 11

Velocity uncertainty

(A3) Two close primaries

As is often the case, two reflectors may be very close together or at times, there may appear two peaks in a low frequency wavelet corresponding to a single reflector. We wish to see the effect of interference on stack power. We consider two close primaries separated by 30 ms at $t_0 = 3s \; and \; t_0' = 3.03s$. The resulting wavelet is shown in Figure 12—we clearly see 2 peaks and that the maximum amplitude has dropped from 1 to 0.8. The effect on stack power is shown in Figure 13.

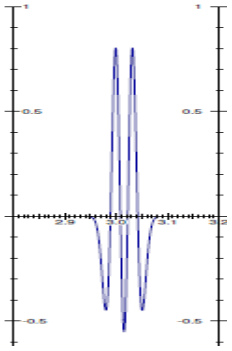

Figure 12

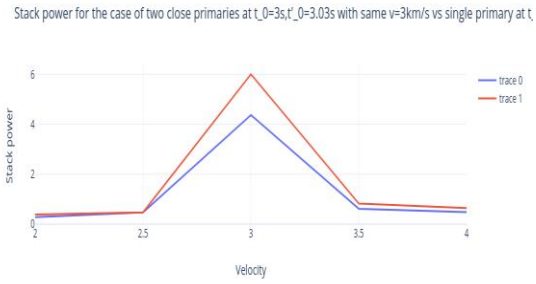

Figure 13

As expected, we see a loss of stack power at all velocities for two close primaries. So, velocity analysis and stacking should be done on properly deconvolved data.

Digressing to an important point—we often assume the amplitude of the peak of a zero phase wavelet to be proportional to the reflection coefficient at the time level, or assume that the ratio of two peaks at 2 reflectors to reflect the ratio of the two reflection coefficients at the two time levels—we see that this is badly disturbed in Figure 14. We started out with two reflectors with reflection coefficients in the ratio of 2:1 say 1 and 0.5, but the resulting amplitudes of the two peaks drop to almost 0.9 and 0.3 i.e. a ratio of 3:1. This further shows the importance of deconvolution.

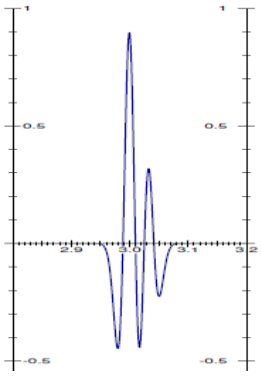

Figure 14

(A4) Primary + Multiple

As is often the case, primary comes mixed with multiple, if multiple attenuation hasn't been done or not done properly before velocity analysis. We consider a primary at $t_0 = 3s, with \; v = 3 \; km/s$ mixed with a surface multiple of primary at $t_0 = 1.5s, with \; v = 2 \; km/s$. Stack power vs. velocity for this case is shown in Figure 15. We see two close peaks at the velocities corresponding to primary and multiple. Obviously, velocity uncertainty is high and we need to be very careful in picking velocity.

Figure 15

Velocity uncertainty

Figure 16

In Figure (16), we have superimposed the stack power of multiple alone (red curve) on the combined stack power of primary and multiple(blue curve)—we see a nice separation of primary and multiple energies, but this may be misleading as we have taken identical frequency content of primary and multiple.

(B) Anisotropic case

We consider the following simple case, where the NMO equation contains an additional 4th order term:-

$$t^2 = t_0^2 + \frac{x^2}{v^2} + \alpha x^4, \qquad (11)$$

where we have added a 4th order correction which may be due to either anisotropy (Leggott et. al, 2000), or ray bending. We take $\alpha = 5 * 10^{-4}$, where x is measured in km and v in km/s. We first try to fit an isotropic velocity i.e. a hyperbola to (11) and calculate stack power vs. velocity and the result is shown in Figure 17—a significant loss of stack power and increase of velocity spread is seen. If we introduce the 4th order term with just 20% of the actual anisotropy parameter i.e. $\alpha' = 10^{-4}$, we see a marked improvement in stack power as well as reduction in velocity uncertainty.

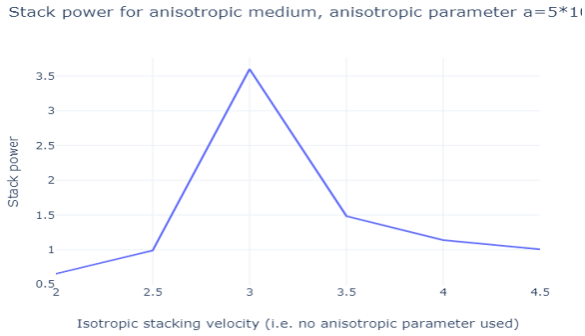

Figure 17

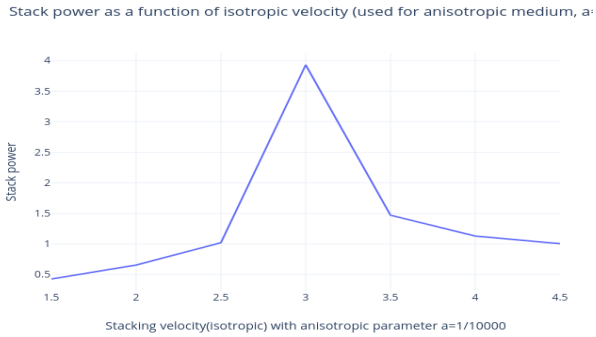

Figure 18

Results with Synthetic Data

We start out with two primaries at zero offset times 1.5s and 3s with velocities 2000 m/s and 3000 m/s respectively. Zero phase Ricker wavelet of duration 200 ms has been used. We see that the primaries cross each other at around 7000 m offset.

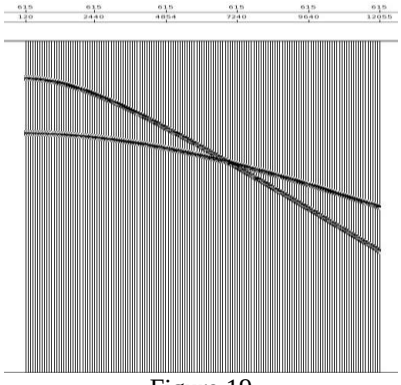

Figure 19

Velocity uncertainty

We first limit offset to 4000 m to avoid noise due to the interference of the two primaries. We maintain the velocity at 1.5 sec to be the correct value of 2000 m/s and vary the velocity at $t_0 = 3s$ from 2800 m/s to 3200 m/s at the interval of 100 m/s. In Figure 20, we show the stacks obtained at these velocities for a hundred CMP's with the central panel being the one with the correct velocity of 3000 m/s. We see that there is some loss of stack power on either side of the correct velocity, but not appreciable enough to allow us to prefer one over the other, at least visually.

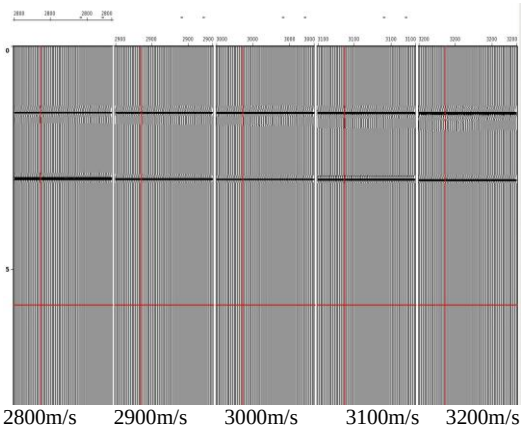

2800m/s 2900m/s 3000m/s 3100m/s 3200m/s

Figure 20

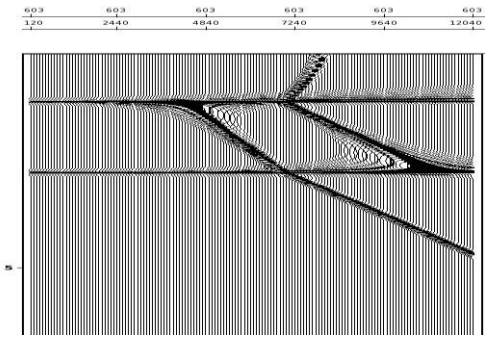

Figure 21

The two primaries in Figure (19) are subjected to NMO with correct velocities at $t_0 = 1.5s \; and \; t_0 = 3s$ for the full offset range of 12040 m and the NMO'ed gather shown in Figure (21). We see that a lot of unwanted noise has been generated. The stacks at velocities from 2800 m/s to 3200 m/s (for the reflector at 3s) at intervals of 100 m/s for the full offset range are shown in Figure 22.

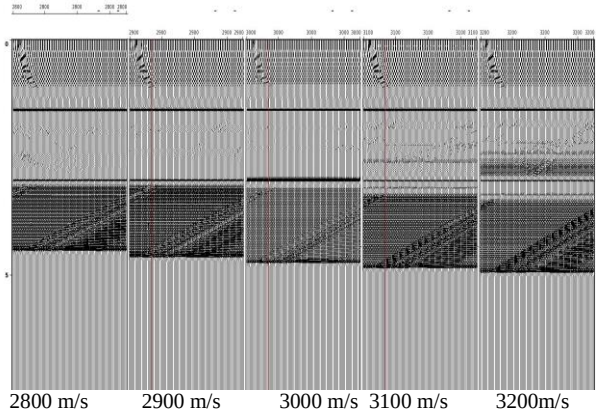

2800 m/s 2900 m/s 3000 m/s 3100 m/s 3200m/s

Figure 22

We see that though a lot of unwanted noise has been generated due to cross-talk between the primaries, velocity discrimination or velocity certainty is much better in this case (of high offset-depth ratio). The highest amplitude for the primary at 3s is seen for the velocity of 3000 m/s and it decays rapidly on either side making velocity discrimination much easier. We next consider the case of a primary at 500 ms with v = 1500 m/s & a primary at 3s with velocity 3000 m/s, as shown in Figure (23). The same is given a constant static shift of 20 ms and a stack generated for 100 CMP's.

Loss of stack power, particularly for the shallow reflector, is evident in Figure (24). In Figure (25), we have included the case of constant static = 50 ms, and see that stack power has almost vanished at both time levels as we had inferred above.

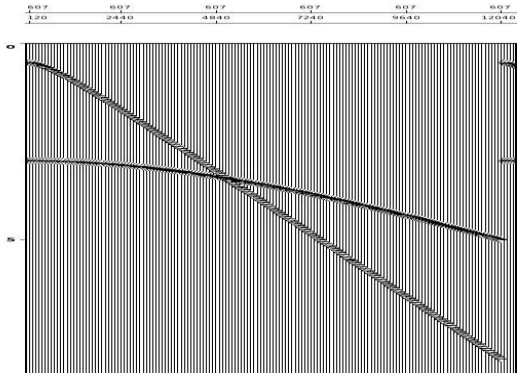

Figure 23

Velocity uncertainty

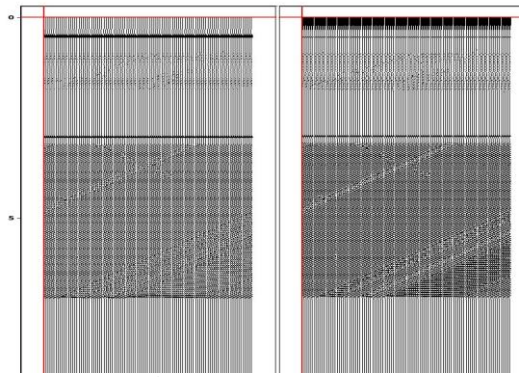

No static shift Constant static=20 ms

Figure 24

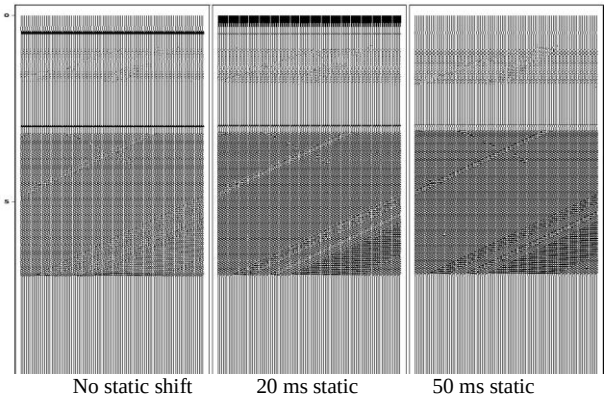

No static shift 20 ms static 50 ms static

Figure 25

We next consider the case of a 1st order surface multiple (of reflector at 1.5s) with velocity 2 km/s, and a primary with velocity 3 km/s, at the same time $t_0 = 3s$, as shown in Figure 26. We first limit the offset to 4000 m and display the stacks obtained at different velocities around the correct primary velocity of 3 km/s(at 3s) in Figure 27.

We see that good enough stacks are obtained for a wide range of velocities ranging from 3300 m/s to multiple velocity of 2000 m/s, making velocity determination difficult. We now increase the offset to 12 km and the results are displayed in Figure 28. We see a better discrimination of velocity at such a high offset-depth ratio, but we also see a great deal of noise added due to cross-talk between the two primaries and multiple.

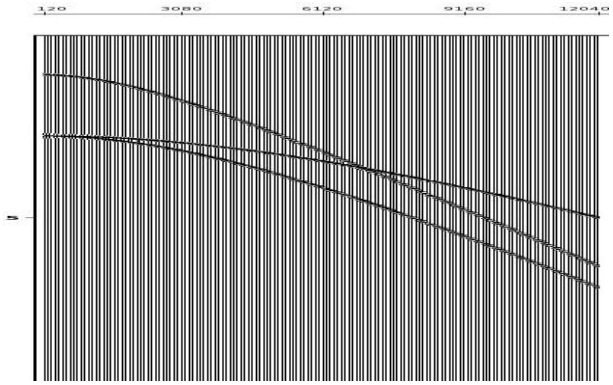

Figure 26

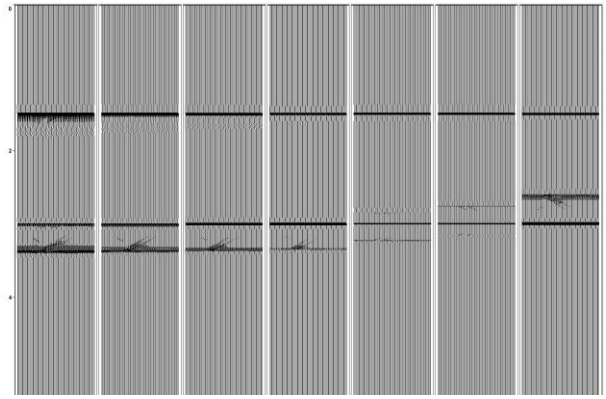

3300m/s 3200m/s 3100m/s 3000m/s 2500m/s 2300m/s 2000m/s

Figure 27

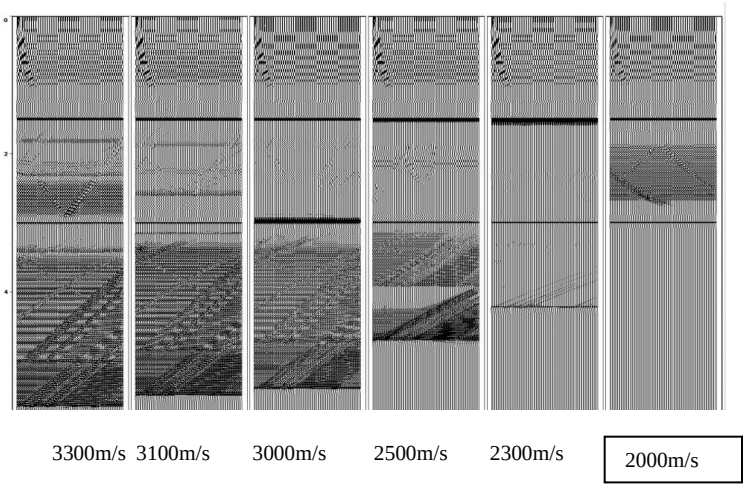

3300m/s 3100m/s 3000m/s 2500m/s 2300m/s 2000m/s

Figure 28

Conclusions

We have studied velocity uncertainty or the uncertainty in our velocity determinations at different time levels and for various offsets. In the isotropic case, we have seen that offset to depth ratio should be high to get reliable estimates of velocity, provided statics are small. The advantage gained by a high offset-depth ratio is offset by statics particularly at shallow depths. We see a rapid loss of stack power with offset at 500 ms, even with statics less than 20 ms. As an extreme example, we have shown that a constant static of 50 ms destroys stack power at all time levels. Floating datum processing or wave equation datuming in such cases is a must.

Stack power vs. velocity was also studied for wavelets with different peak frequencies—surprisingly, this only led to minor changes. We have also analyzed the case of two close primaries and seen that their interference affects stack power adversely. Deconvolution, in such cases, should be done not only to resolve the primaries, but also to get stacks with greater stand-outs.

We also studied velocity uncertainty for the case of a primary mixed with a multiple of lower velocity at the same zero offset time. We found that velocity estimation in such cases is difficult, particularly for low offset to depth ratios. High offset to depth ratio does benefit velocity discrimination significantly, but introduces a lot of unwanted noise. Finding effective ways to tackle such noise will certainly add value, provided we can keep our static values quite low when we are dealing with high offset data.

Finally, we also looked at the anisotropic case and found that fitting an isotropic velocity to a curve with even a small 4^{th} order term is detrimental to the stack. On the other hand, if we introduce just a fraction of the actual anisotropy parameter in our equation, not only does stack power improve, but velocity uncertainty also reduces significantly. So whenever we are dealing with high offsets, and ray bending or anisotropy becomes significant, we must go for higher order corrections in our velocity analysis.

References

Ricker, N., 1943, Further developments in the wavelet theory of seismogram structure: Bulletin of the Seismological Society of America, 33, 197–228.

Ricker, N., 1944, Wavelet functions and their polynomials: Geophysics, 9, 314–323, doi: 10.1190/1.1445082.

Leggott, Richard & Cheadle, Scott & Whiting, Peter & Williams, R., 2000, Analysis of higher order moveout in terms of vertical velocity variation and VTI anisotropy: Exploration Geophysics - EXPLOR GEOPHYS. 31. 10.1071/EG00455.

Acknowledgments

The author expresses his sincere thanks to Director (E), ONGC Ltd for his permission to publish this paper. The author is also grateful to Shri H. Madhavan, GGM,-Basin manager, Western onshore basin and Shri Matibar Singh, GGM-Head Geophysical Services, Vadodara for their encouragement and support. The author is indebted to Shri Rajesh Madan, CGM-Head RCC, Vadodara for useful suggestions.